HAL open science

Linking Ocean Forcing and Atmospheric Interactions to Atlantic Multidecadal Variability in MPI-ESM1.2

J. Oelsmann, Leonard F. Borchert, R. Hand, Johanna Baehr, Johann Jungclaus

To cite this version:

J. Oelsmann, Leonard F. Borchert, R. Hand, Johanna Baehr, Johann Jungclaus. Linking Ocean Forcing and Atmospheric Interactions to Atlantic Multidecadal Variability in MPI-ESM1.2. Geophysical Research Letters, 2020, 47 (10), pp.e2020GL087259. 10.1029/2020gl087259 . hal-03147378

HAL Id: hal-03147378

https://hal.science/hal-03147378v1

Submitted on 21 Feb 2021

HAL is a multi-disciplinary open access archive for the deposit and dissemination of scientific research documents, whether they are published or not. The documents may come from teaching and research institutions in France or abroad, or from public or private research centers.

L'archive ouverte pluridisciplinaire **HAL**, est destinée au dépôt et à la diffusion de documents scientifiques de niveau recherche, publiés ou non, émanant des établissements d'enseignement et de recherche français ou étrangers, des laboratoires publics ou privés.

Distributed under a Creative Commons Attribution 4.0 International License

Check for updates

AGU100 ADVANCING EARTH AND SPACE SCIENCE

Geophysical Research Letters

RESEARCH LETTER
10.1029/2020GL087259

Linking Ocean Forcing and Atmospheric Interactions to Atlantic Multidecadal Variability in MPI-ESM1.2

J. Oelsmann[1,2], L. Borchert[1,3,4], R. Hand[1,5,6], J. Baehr[3], and J. H. Jungclaus[1]

[1]Max Planck Institute for Meteorology, Hamburg, Germany, [2]Deutsches Geodätisches Forschungsinstitut der Technischen Universität München, Munich, Germany, [3]Institute for Oceanography, Center for Earth System Research and Sustainability (CEN), Universität Hamburg, Hamburg, Germany, [4]Sorbonne Universités (SU/CNRS/IRD/MNHN), LOCEAN Laboratory, Institut Pierre Simon Laplace (IPSL), Paris, France, [5]Geographical Institute, University of Bern, Bern, Germany, [6]Oeschger Centre for Climate Research, University of Bern, Bern, Germany

Key Points:
- Multidecadal AMOC variations drive extratropical SST variations in idealized model simulations
- Associated ocean heat release synchronizes atmospheric circulation anomalies that amplify basin-wide warming related to AMV
- Timescale of persistence and phenomenology of monopole AMV-SLP/SST responses are controlled by ocean dynamics in idealized model simulations

Supporting Information:
- Supporting Information S1

Correspondence to:
J. Oelsmann,
julius.oelsmann@tum.de

Citation:
Oelsmann, J., Borchert, L., Hand, R., Baehr, J., & Jungclaus, J. H. (2020). Linking ocean forcing and atmospheric interactions to Atlantic multidecadal variability in MPI-ESM1.2. *Geophysical Research Letters*, *47*, e2020GL087259. https://doi.org/10.1029/2020GL087259

Received 29 JAN 2020
Accepted 24 APR 2020
Accepted article online 29 APR 2020

©2020. The Authors.
This is an open access article under the terms of the Creative Commons Attribution License, which permits use, distribution and reproduction in any medium, provided the original work is properly cited.

Abstract We investigate how ocean-driven multidecadal sea surface temperature (SST) variations force the atmosphere to jointly set the pace of Atlantic multidecadal variability (AMV). We generate periodic low-frequency Atlantic Meridional Overturning Circulation oscillations by implementing time-dependent deep-ocean-density restoring in MPI-ESM1.2 to explicitly identify variations driven by Atlantic Meridional Overturning Circulation without any perturbation at the ocean-atmosphere interface. We show in a coupled experiment that ocean heat convergence variations generate positive SST anomalies, turbulent heat release, and low sea level pressure in the subpolar North Atlantic (NA) and vice versa. The SST signal is communicated to the tropical NA by wind-evaporative-SST feedbacks and to the North-East Atlantic by enhanced northward atmospheric heat transport. Such atmospheric feedbacks and the characteristic AMV-SST pattern are synchronized to the multidecadal time scale of ocean circulation changes by air-sea heat exchange. This coupled ocean-atmosphere mechanism is consistent with observed features of AMV and thus supports a key role of ocean dynamics in driving the AMV.

Plain Language Summary The Atlantic multidecadal variability is an observed fluctuation of North Atlantic ocean surface temperatures on multidecadal time scales. It strongly influences climatic conditions over the surrounding continents in the North Atlantic region as well as in remote areas. Therefore, it is essential to understand the underlying mechanisms, particularly in regard to predict the Atlantic multidecadal variability itself and its impacts. However, the respective contributions from fast atmospheric forcing and slow ocean variations to such long-term climate variations have been controversially discussed. Here, by artificially increasing the variability of ocean dynamics in a climate model, we improve the mechanistic understanding of the role of ocean dynamics in driving the Atlantic Multidecadal Variability. We believe our results suggest a major role for ocean dynamics. A climate model reacts to an increase in ocean circulation by accumulating heat in the subpolar North Atlantic. Associated atmospheric responses to ocean forcing contribute to heat redistribution to form the basin-wide sea surface temperature pattern of Atlantic Multidecadal Variability. None of these fundamental imprints of ocean dynamics can be reproduced by a model experiment that excludes ocean dynamics (slab-ocean model). Our results therefore substantiate Atlantic multidecadal variability as a coupled mode of ocean-atmospheric variability, which strongly relies on the slow circulation variations of the ocean.

1. Introduction

Currently, no consensus exists on the drivers of Atlantic multidecadal variability (AMV). AMV is associated with coherent, multidecadal fluctuations of North Atlantic (NA) sea surface temperatures (SSTs) and was discussed to be driven by a combination of internal climate variability of the ocean and the atmosphere as well as by external forcings (e.g., Booth et al., 2012; Schlesinger & Ramankutty, 1994; Zanchettin et al., 2014). The internally generated proportion of AMV was conventionally viewed to be controlled by multidecadal variations of the Atlantic Meridional Overturning Circulation (AMOC) (Delworth et al., 1993; Danabasoglu, 2008; Knight, 2005). This point of view was, however, challenged by Clement et al. (2015), arguing that AMV might be a result of atmospheric-ocean-mixed-layer interactions. The individual roles of ocean dynamics or atmospheric forcing in shaping AMV remain thus controversial. Here, we improve the mechanistic

understanding of those fundamentally different dynamics to shed light on the underlying components of internal AMV.

Numerous studies have supported the role of ocean dynamics as the central pacemaker of AMV (Delworth et al., 2017; Zhang et al., 2016). The AMOC, which conveys heat to high latitudes in the NA regions, was indicated to exhibit enhanced multidecadal variability by several model-based studies (Ba et al., 2013; Delworth & Greatbatch, 2000; Jungclaus et al., 2005). Such long-term anomalies were suggested to primarily originate from changes in deep water formation rates in the Labrador Sea and by the overflows (Ba et al., 2014; Delworth et al., 1993). Zhang and Zhang (2015) showed that, as a response to strong subpolar NA density perturbations, the resulting southward propagating advective signals were accompanied by ocean heat convergence in the subpolar gyre (SPG) and heat divergence in the Gulf Stream region. This oceanic redistribution of heat and salinity was linked to the characteristic AMOC subsurface dipolar temperature and salinity fingerprint, which, consistent with long-term AMOC variability, was characterized by multidecadal time scales of persistence. In a subsequent study, Zhang (2017) underpinned that these features associated with long-term AMOC variability were unequivocal properties of emergence of AMV. Based upon this dynamical ocean mechanism, Borchert et al. (2018) found predictive skill in the NA region several years ahead, which was potentially linked to enhanced time scales of persistence of SSTs under oceanic forcing. As a result, several indicators exist for an ocean-driven AMV.

In contrast to the dynamic ocean-driven mechanism, Clement et al. (2015) put forward stochastic atmospheric forcing as a sufficient driver of AMV. They argued that extratropical forcing of the North Atlantic Oscillation (NAO) and related thermodynamic coupling in the tropics drive associated NA-SST variations (Clement et al., 2015; Gastineau & Frankignoul, 2015). In this context, Cane et al. (2017) showed that slab ocean or even more simplified process models can reproduce red-noise AMV characteristics, owing to the dampening time scale of the upper mixed layer of the ocean. From that perspective, the ocean was not considered as an active component of the AMV.

The ambiguity of the internal sources of AMV further encouraged investigations on the phenomenology of AMV and its low-frequency climate signatures (O'Reilly et al., 2016; Zhang, 2017; Zhang et al., 2016). In particular, the importance of anomalous extratropical surface heat transfer on multidecadal time scales to assert ocean dynamics as the driving force was discussed (Cane et al., 2017; Gulev et al., 2013; O'Reilly et al., 2016; Zhang et al., 2016). O'Reilly et al. (2016) suggested that positively correlated SSTs and surface heat flux (SHF) release thereafter indicate ocean forcing, while negative correlations are an attribute of interannual atmospheric variability. Although this rationale conceptually fits to subpolar ocean heat accumulation as described by Zhang and Zhang (2015), the interpretation of Gulev et al.'s (2013) results was questioned by Cane et al. (2017), arguing that directionality of SHFs can be an artifact of low-pass filtering and thus not explicitly identify AMV as a response to AMOC variability.

Here, we aim to explicitly link multidecadal AMOC variability to SHF release and to elucidate how AMOC variations connect to the basin-wide SST-pattern associated with AMV. Therefore, we construct idealized experiments, to determine the influence of AMOC variations on regional SSTs, SHFs, and ultimately the AMV. Our method is inspired by a setup used in Delworth and Zeng (2016), who forced different climate models with NAO related heat flux perturbations to drive long-term AMOC anomalies. In their setup, coupled ocean-dynamics-resolving models indicated a basin-wide SST response following strong NAO-heat-flux forcing with a decadal scale lag, which was not found in a slab-ocean configuration (Delworth et al., 2017). Thus, the authors underlined the potential role of the AMOC in driving the AMV, by enhanced northward heat transport as a response to the imposed buoyancy forcing. Motivated by their results, we extend Delworth et al.'s (2017) approach by applying time-dependent deep-ocean-density restoring in coupled and ocean-only configurations. With this approach we avoid the direct manipulation of SHFs by the forcing itself and yet produce similar low-frequency AMOC modulations, as under NAO forcing.

We enhance understanding of the dynamic ocean mechanism by revealing how the ocean synchronizes atmospheric feedbacks to jointly cause the basin-wide AMV response. We show that multidecadal time scales of persistence of SSTs can only be provided by low-frequency ocean forcing and not by stochastic atmospheric mixed layer interactions. The results thus substantiate AMOC variations as the central driver of AMV in our model experiments.

2. Methods and Experimental Setup

We perform four different sets of experiments to assess AMOC-driven SST variations and corresponding responses of the atmospheric circulation to those ocean forced modulations. Thereto, we use a hierarchy of model setups of the Max-Planck-Institute Earth System Model-LR (MPI-ESM1.2-LR, Mauritsen et al., 2019, Version 1.2). The atmospheric component of MPI-ESM-LR horizontally features a spectral truncation at T63/1.9° resolution (approximately 200 km grid spacing) and 47 hybrid sigma—pressure levels (Giorgetta et al., 2013). The curvilinear bipolar grid of the ocean component has a nominal resolution of 1.5° (with roughly 25 to 100 km resolution in the subpolar North Atlantic) and 40 z-levels.

We perform different experiments in either the coupled, ocean-only and slab ocean configurations. We additionally include a corresponding coupled preindustrial simulation (400 years) as a reference integration. All experiments feature constant external forcing (greenhouse gas concentrations and orbital parameters) with prescribed seasonal but no interannual variability.

2.1. Coupled NAO-Heat-Flux Experiment: CPL-HEAT-FLUX

The basic idea behind our experimental setup is that we artificially drive anomalous, multidecadal phases in the AMOC to clearly identify the actively ocean-driven responses. Thus, in the first experiment we reproduce the heat-flux forcing method as applied by Delworth and Zeng (2016) in the coupled model configuration. The NAO-related heat fluxes are utilized as a buoyancy forcing in the subpolar NA to drive anomalous overturning (Delworth & Greatbatch, 2000; Eden & Jung, 2001). The associated forcing pattern is obtained from regressing monthly net air-sea heat flux anomalies onto the normalized NAO index in the preindustrial run. The NAO is derived from the principal components of the first empirical orthogonal function of winter (December–March) sea level pressure (SLP) anomalies in the region 90°W to 40°E and 0 °–90°N. As in Delworth and Zeng (2016), we add those monthly mean heat flux perturbations to the daily computed heat flux balance only in winter (December–March) with a linear ramping in November and April. The heat flux forcing is spatially confined to 90°W to 60°E and 20–80°N and given in the supporting information Figure S4. We modulate this forcing with a period of 40 years between ±2 standard deviations NAO, which is of comparable magnitude to the forcing used by Delworth and Zeng (2016) and yields strongest AMOC anomalies. This experiment is thereafter called CPL-HEAT-FLUX. Because the implemented NAO SHF forcing affects both, ocean and atmosphere, the experimental setup restricts investigations on the purely AMOC-driven atmospheric responses. Thus, we construct a similar modified setup without affecting the atmospheric model component directly.

2.2. Coupled Thermohaline-Restoring Experiment: CPL-TH-REST

This second experiment features subsurface thermohaline density restoring in the subpolar NA. Here, we use the anomalies which are produced by the NAO forcing in the ocean interior to create similar density gradients and to cause anomalous AMOC modulations as in CLP-HEAT-FLUX. Hence, in this setup we particularly avoid direct modification of SHFs and SSTs by the forcing. The density anomalies are computed from composites of monthly temperature and salinity anomalies that correspond to a full NAO-forcing-cycle of 40 years from the CPL-HEAT-FLUX experiment. We then progressively restore three-dimensional T and S fields to this composite with a temporal relaxation coefficient of 20 days. As we confine the restoring horizontally to the subpolar NA and to below 700 m we do not affect the atmosphere directly. This method is applied in the coupled (CPL-TH-REST) configuration.

2.3. Ocean-Only Thermohaline-Restoring Experiment: OM-TH-REST

In the third experiment we additionally implement the same density restoring as in CPL-TH-REST in a standalone ocean-model (OM-TH-REST), which is based on MPIOM6.3 (Jungclaus et al., 2013). This stand-alone setup is designed to distinctively identify AMOC controlled SST variations, as here the atmosphere cannot respond to any changes in the ocean circulation or feed back onto SSTs. The ocean model is forced with sets of atmospheric fluxes that are derived from randomly selected 1-year blocks of the analogous preindustrial control integration. In that way we mimic atmospheric white-noise-like forcing without serial correlation on annual time scales.

2.4. Slab-Ocean Experiment: SLAB-OM

The fourth experiment (SLAB-OM) is the complement to the slab-ocean experiment by Clement et al. (2015) and based on the atmospheric model Echam-6.3.04. This atmosphere module is coupled to a 50-m-deep slab ocean, with prescribed climatological ocean heat transport.

Table 1
List of Experiments

Experiment	Forcing	Configuration	Member	Duration
CPL-HEAT-FLUX	40 years periodic NAO-HF forcing	coupled	5	400 years
CPL-TH-REST	40 years periodic T-S restoring	coupled	5	400 years
OM-TH-REST	40 years periodic T-S restoring	ocean only	5	400 years
SLAB-OM	preindustrial	slab ocean	1	300 years

Each dynamic-ocean experiment (CPL-HEAT-FLUX, CPL-TH-REST, and OM-TH-REST) comprises five ensemble members, which are started from different times of the control integration (separated by 20 year intervals). The coupled simulations have a length of 400 years and the ocean-only experiment covers 300 years. The SLAB-OM experiment consists of one run of 300 years (Table 1).

2.5. Statistical Testing and Variables

In the following we consider anomalies as the annual ensemble mean departures from the respective ensemble temporal mean and avoid any further low-pass filtering of the data (Cane et al., 2017). The AMV index is computed as the spatially averaged SSTs over the area 0°–60°N and 80°W to 0° consistent with Clement et al. (2015) and Frankignoul et al. (2013). AMOC is quantified by the maximum Atlantic meridional streamfunction at 45°N and 26°N in z-space. We use both indices to illustrate its temporal relation with AMV.

We determine statistical significance of point-wise (lead-lag) correlation maps by permutation tests. First, we calculate the correlation coefficient r after Pearson (r). Then at every grid point, we randomize one of the time series $n = 3,000$ times, from which the permuted correlation coefficients r_p were computed. By assuming that the null hypothesis $H_0 : r = r_p$ is true, the so computed r_p constitute the permutation distribution. Using this distribution, we numerically compute p values for the observed correlations r. The two-sided p values are derived as $p = P(r_p > |r|) + P(r_p < -|r|)$. We specify a significance level $\alpha = 0.05$ and reject the null hypothesis when $p \leq \alpha$. To account for multiplicity (e.g., Wilks, 2006, 2016), we apply the procedure of Benjamini and Hochberg (1995) to control the false discovery rate (FDR). This approach ensures that FDR<= α_{FDR}; that is, it sets an upper limit to the ratio of the erroneous rejections of the null hypothesis (α error) and the total rejections. We chose $\alpha_{FDR} = 0.05$, but note that it does not necessarily be equal to the local significance level α. We use the "multipletest" routine of the Python module statsmodels.

3. Phase Locking of AMV With AMOC

Our model simulation reproduces stable AMOC oscillations (Figure 1a) from NAO heat flux forcing, as found in CM2.1 (Delworth & Zeng, 2016). We obtain analogous results when we only adjust the deeper density field in the subpolar ocean in coupled or ocean-only configurations (Figures 1b and 1c). AMV is notably phase locked to the imposed periodic oscillations with a lag of about 5 years with respect to $AMOC_{45N}$ in the coupled experiments (CPL-HEAT-FLUX and CPL-TH-REST). AMOC-AMV coupling indicates to be a result of the ocean mechanism promoted by Zhang (2017), supporting the important role of the AMOC as the pacemaker. This dependency is, however, much reduced in the ocean-only model (OM-TH-REST), where atmospheric feedbacks are switched off. Here, AMV does not fully reproduce amplitude and periodicity as seen in CPL-TH-REST, implying that atmospheric coupling plays an essential role in the ocean mechanism in the coupled experiment. As in Zhang (2017), low-frequency ocean-driven AMV variations differ from its behavior in the case of no ocean circulation variability in the slab-ocean variant. In this setup, AMV is characterized by higher power on interannual and subdecadal time scales (Figure 1d) than in the fully coupled variants.

We analyze regression maps of SST anomalies associated with either AMV or $AMOC_{26N}$ changes (Figure 2). The patterns are given at Lag 0, because AMV and $AMOC_{26N}$ are found to be in phase in the coupled experiments. SST regression maps for the coupled heat flux and restoring runs are almost indistinguishable when either regressing onto AMV or $AMOC_{26N}$ (Figures 2a and 2d, and 2b and 2e). We find strong coherence of maximum SPG warming, the tropical branch and a cooling patch in the Gulf Stream region.

Responses in OM-TH-REST, however, differ substantially from its coupled counterpart (Figure 2f). Considering that this ocean stand-alone excludes any atmospheric responses to ocean variability, we identify the resulting SST pattern as the surface fingerprint of the AMOC. No atmospheric forcing can cause this

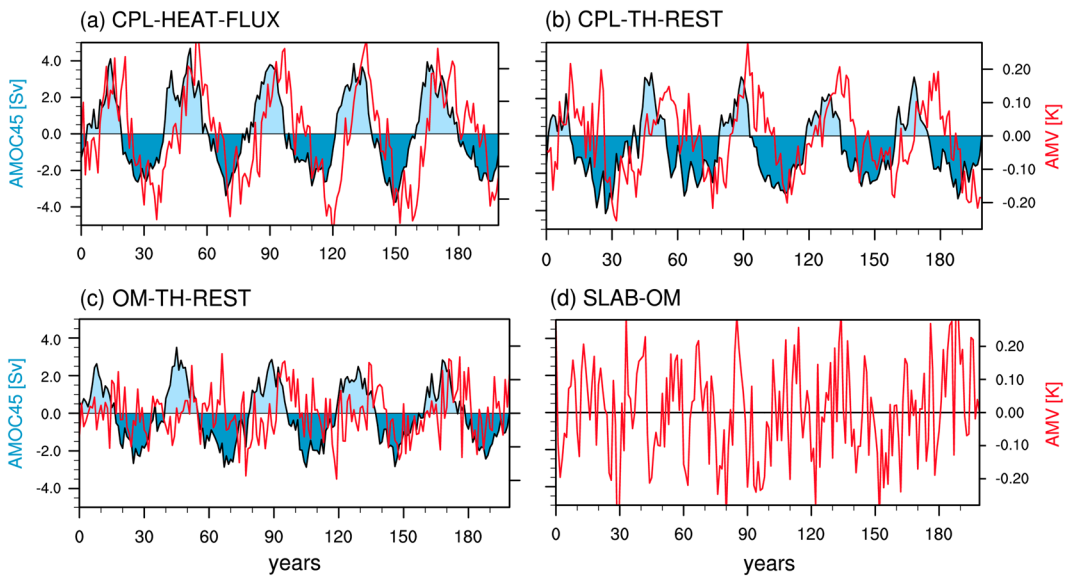

Figure 1. Evolution of maximum annual anomalies of AMOC at 45°N (blue, in Sv) showing the first 200 years of integration for the experiments including ocean dynamics (a–c). AMV index (red, in K) denotes annual mean SST anomalies averaged over 0°–60°N and 80°W to 0°. AMV index for SLAB-OM is shown in (d).

long-term response, because the applied stochastic atmospheric forcing is averaged out by the ensemble mean. Conclusively, in this setup any SST changes reflect what is directly driven by the ocean circulation. The differences (in particular the tropical/subtropical warming in the coupled variant) must be caused and amplified by atmospheric responses to ocean forcing. Atmospheric dynamics are critical for the full response, which is underpinned by the much reduced AMOC-AMV correlation in the ocean-only setup as visualized by the time series (Figure 1d).

We observe different AMV-related SST responses between the coupled experiment (heat flux or restoring, Figures 2a and 2b) and the SLAB-OM experiment (Figure 2c), particularly in the extratropics. Characteristic features, such as the SPG-Gulf Stream SST-dipole in the coupled runs, are not present in the mixed-layer setup. In SLAB-OM we observe a tripolar SST pattern, which was frequently linked to NAO forcing (Delworth et al., 2017; Trenberth & Zhang, 2019; Wills et al., 2019). Clement et al. (2016) argued that this SST pattern (Figure 2c) would be largely consistent with observed AMV and not significantly altered when allowing for ocean variability in a coupled simulation. However, our setup provides strong indications that AMV in the coupled experiments is not generated by the same mechanism as in SLAB-OM in mid-latitudes. Phase locking of AMOC and AMV (Figures 1a and 1b) and the evident AMOC surface expression (Figure 2f) point to a possible influence of the ocean in driving AMV in the mid-latitudes. It is thus crucial to further understand the differences in the mechanisms, which cause AMV in the coupled or atmosphere-only experiments. With the focus on both components, the ocean and the atmosphere, we strive to determine which of those mechanisms provides a more coherent picture with observed signatures of AMV. To specify the contribution of ocean forcing, we analyze how ocean heat convergence controls spatiotemporal characteristics of SST responses and how those responses differ in the SLAB-OM experiment.

4. The AMOC-SST Fingerprint

We identify the same underlying processes causing the dipolar AMOC-SST fingerprint as for the subsurface responses found in Zhang and Zhang (2015) by showing lead-lag correlations of ocean heat transport, ocean heat convergence and SSTs with respect to $AMOC_{26N}$ (Figures 3a–3i).

All dynamic-ocean experiments similarly indicate slow southward propagation of ocean heat transport anomalies in the subpolar region and quick communication to the southern Atlantic south of 35°N (Figures 3a–3c), which is in line with many previous studies (Borchert et al., 2018; Hand et al., 2020; Zhang & Zhang, 2015). At Lag 0 we show that net meridional ocean heat transport variations cause positive ocean heat convergence anomalies in the SPG region and heat divergence south of it, with a slight maximum at

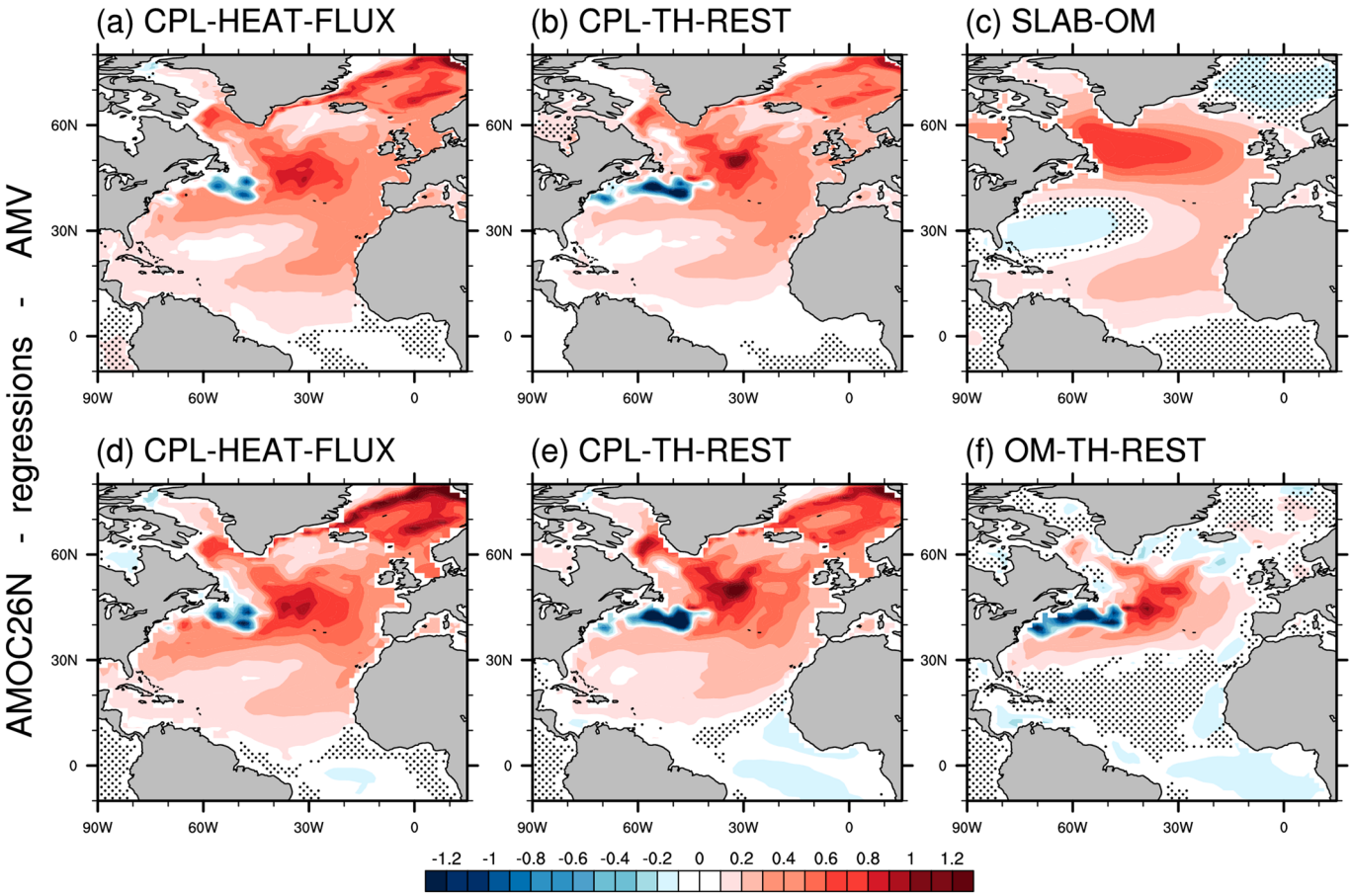

Figure 2. Upper panel (a–c) shows annual SSTs (shading, K) associated with a change of 1 standard deviation AMV at Lag 0 for coupled and slab-ocean experiments. Equivalently, regressions on 1 standard deviation change of the $AMOC_{26N}$ are given in the lower panel (d–f) for all experiment indcluding ocean dynamics. Stippling denotes regions where SST regressions are not significant (section 2.5).

the Gulf Stream latitude (Figures 3d–3f). In the ocean-only experiment (OM-TH-REST), ocean-driven heat accumulation match exactly the SST responses given in the third panel (Figures 3f and 3i).

Again, as shown in the SST regression maps (Figures 2d and 2e), we find enhanced significant spatial coverage of the warming signal in the coupled experiments extending further south to about 10°N (black boxes in Figures 3g and 3h). However, positively correlated SSTs (with AMOC anomalies) coincide with regions that are actually affected by ocean heat extraction in the tropics and subtropics (10°–30°N). Because this tropical branch is not seen in OM-TH-REST, we argue that this opposing response is due to additional redistribution of heat, which must be accomplished by the atmosphere. As this tropical signal has the same time scale of AMOC modulations either in the heat flux or restoring experiment, atmospheric circulation anomalies are consequently as well phase locked to those multidecadal AMOC variations.

We show indications that the mechanisms causing the basin-wide AMOC-SST response in the coupled simulations also apply for AMV development in our setup. In agreement with the AMOC/AMV-SST regression maps (Figure 2), spatiotemporal features given in the lead-lag correlation SST maps either referring to AMV or AMOC comply very well in the coupled simulations (Figures 3j and 3k). Hence, AMOC variations are largely responsible for the low-frequency NA-SST variations related to AMV in the experiments with dynamic ocean circulation. Ocean heat convergence explains emergence of the AMOC fingerprint in the OM-TH-REST setup and thus confirms the SPG region as the hot spot of ocean-driven heat release to the atmosphere. Different mechanisms cause AMV in the slab-ocean experiment. Here, NAO-related heating/cooling is reflected by the tripolar SST pattern of short (subdecadal) persistence as shown in Figure 3l. Previous studies showed, however, that this short time scale of persistence in slab-ocean or red-noise models (Li et al., 2020; Zhang, 2017) strongly underestimates the observed multidecadal time scale of AMV-NASSTs.

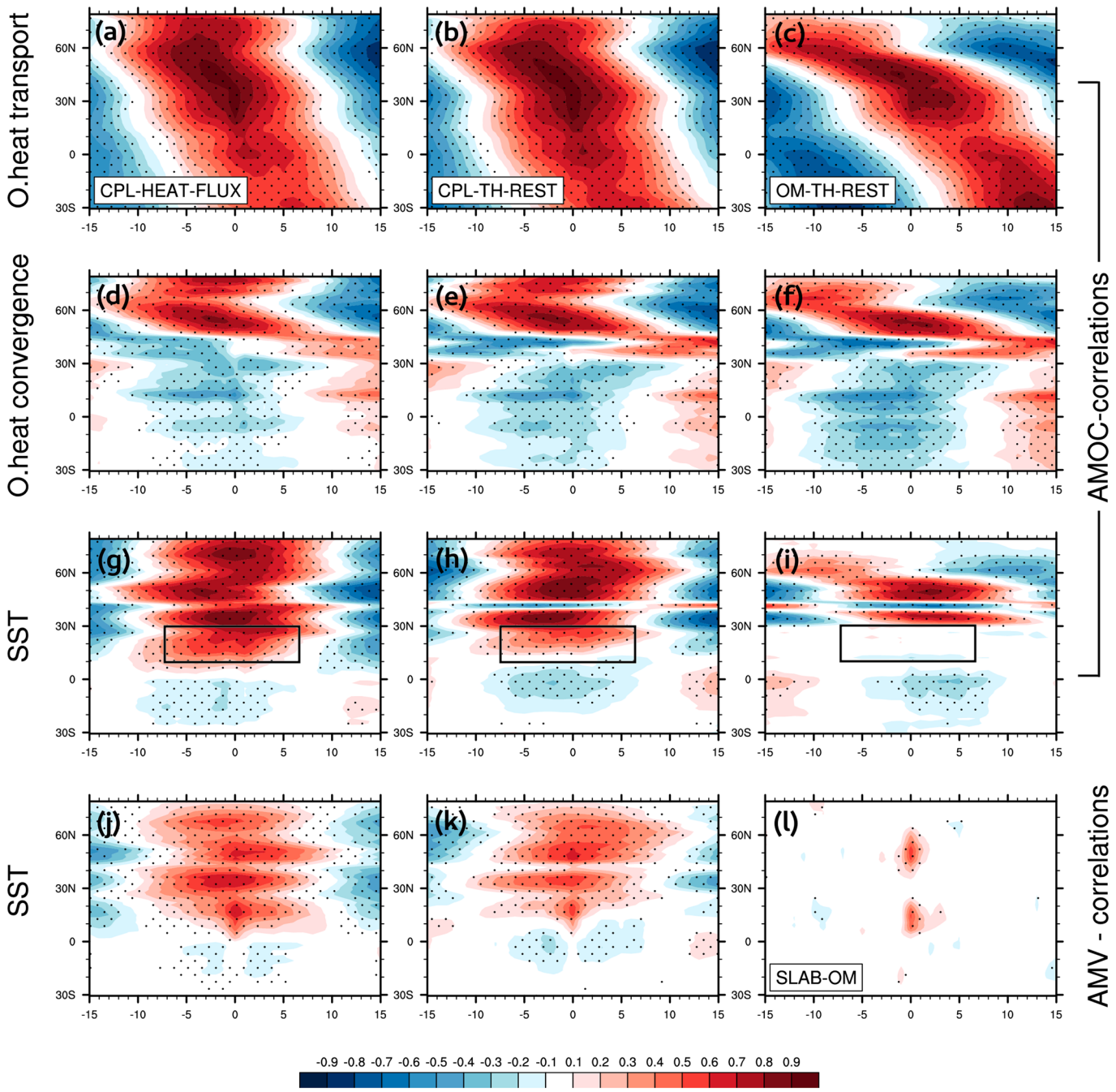

Figure 3. Lead-lag cross-correlation coefficients of annual averaged Atlantic ocean heat transport (a–c), ocean heat convergence (d–f), and SSTs (g–i) with respect to $AMOC_{26N}$ (and AMV, j–l). Black boxes highlight the different tropical SST responses across the coupled and ocean-only experiments. Negative/positive years denote when AMOC/AMV lags/leads. Oceanic key features are given for CPL-HEAT-FLUX, CPL-TH-REST, and OM-TH-REST. Note that the lower right plot refers to the SLAB-OCEAN experiment (l). Stippling indicates statistical significance based on the 5% global level (section 2.5).

It was also demonstrated that the temporal evolution and characteristics of SSTs and ocean-atmosphere fluxes produced in coupled simulations are more consistent with observations than are those from a slab-ocean experiment (e.g., Figure 12 in Wills et al., 2019). Our modeling results provide evidence that ocean dynamics can explain enhanced persistence at low-frequency and observed lead-lag relationships of ocean-atmosphere fluxes. The importance of ocean heat transport as a source of decadal NA-SST prediction skill (Borchert et al., 2019) further supports this link between ocean-forcing and AMV.

Given the similarity of the responses in CPL-HEAT-FLUX and the CPL-TH-REST, we further underpin Delworth and Zeng's (2016) results and are able to study unperturbed (by the forcing) atmospheric responses in the CPL-TH-REST run. In the following we restrict our analysis to the coupled restoring experiment and show regression maps with respect to AMV, because key features like SSTs, SHFs, atmospheric anomalies, and time scale of persistence are very similarly correlated with $AMOC_{26N}$.

5. Contributions of Synchronized Atmospheric Feedbacks to AMV

The characteristic atmospheric circulation pattern in CPL-TH-REST and SLAB-OM pronounces the substantial different nature of AMV under active ocean or stochastic atmospheric forcing. The dipolar SLP anomaly and easterly midlatitude wind anomalies in the SLAB-OM experiment (Figure 4d) indicate negative NAO conditions for a positive AMV phase. Associated tripolar extratropical heat fluxes lead AMV by one year and cause the previously described tripolar SST response, also shown by Zhang et al. (2016) and O'Reilly et al. (2016). Contrary to that, in the coupled run, a monopole low SLP anomaly east of maximum warming and corresponding cyclonic atmospheric rotation at the surface evolve (Figure 4e). These anomalous atmospheric conditions (SLP) are tightly linked to SHF release in the SP ocean (Figure 4b). Both the extratropical SLP pattern and SHF release clearly differ from the NAO conditions in the slab-ocean variant and illustrate the mismatches of the prevailing mechanisms of AMV in the setups. The large-scale low SLP pattern in CPL-TH-REST much better resembles the observed basin-wide low SLP anomalies, either based on the comparison of long-term differences between positive and negative AMV phases (Sutton & Hodson, 2005), on low-frequency component analysis (Wills et al., 2019), or based on regressions on the low-pass filtered (11-year running mean) AMV index (supporting information Figure S2). Neither the annual nor the low-pass-filtered SLP regressions in SLAB-OM can explain the observations, as they constantly reflect the dipolar SLP structure (supporting information Figures S2g and S2h).

While these findings further substantiate a key role of ocean dynamics, the previously shown differences between the AMV-SST pattern in the coupled and the ocean-only model suggest that atmospheric feedbacks represent an integral part in amplifying the ocean-driven signal. We explore further how the atmospheric processes are intertwined with ocean forcing and contribute to AMV in the fully dynamic coupled setup.

Turbulent heat release from the ocean to the atmosphere in the subpolar NA (Figure 4b) marks the gateway of oceanic forcing. We are able draw this direct link of AMOC variations to those heat flux anomalies, because the SHFs spatially reflect the dipolar SST pattern found in the OM-TH-REST experiment (Figure 2f), as well as areas of ocean heat convergence (Figures 3d–3f). Observational (Gulev et al., 2013) and modeling studies (e.g., O'Reilly et al., 2016; Zhang, 2017; Zhang et al., 2019) substantiated the multidecadal coherence of SHF release during a positive AMV phase. Such dependency exists also in the unperturbed control-simulation of MPI-ESM1.2 (supporting information Figure S1). With our setup, we are in a unique position to confirm this relationship as a central element of ocean forcing.

A low SLP anomaly and low-level convergence develops as a response to ocean-driven midlatitude diabatic heating (Figure 4e), which agrees well with previous process studies (Ghosh et al., 2017; Hoskins & Karoly, 1981; Kushnir, 1994; Kushnir & Held, 1996). The low SLP anomalies not only develop downstream of the maximum SSTs and SHF release but also expand to the tropics. In these tropical/subtropical regions (here south of 30°N), we find mostly positive heat flux anomalies (into the ocean), which either additionally increase SSTs and/or atmospherically compensate meridional ocean heat divergence (Figure 4b). We argue that this southward low SLP extension is sustained by atmospheric thermodynamic coupling with the upper mixed layer. We propose that associated enhancement of SSTs in the tropical arm of the AMV is caused by two major atmospheric feedback mechanisms.

The southward propagation of SLP, SST, and northwesterly wind anomalies is facilitated by the wind-evaporative-SST (WES) feedback effect, as described in earlier studies (Chiang & Bitz, 2005; Xie & Philander, 1994; Xie & Carton, 2013). Oceanic extratropical heating drives anomalous southward SLP gradients and thereafter northerly wind anomalies (see Figure 4e, box) that are deflected eastward by the Coriolis force. Associated weakening of trade winds reduces evaporation, as indicated by the P-E and surface wind speed maps in Figure 4f (black box), which increases latent warming in the tropics/subtropics (Figure 4b). The WES feedback effect has also been proposed to produce the tropical branch as a response to NAO forcing (Clement et al., 2015; Czaja et al., 2002; Gastineau & Frankignoul, 2015); it thus allows for an explanation of

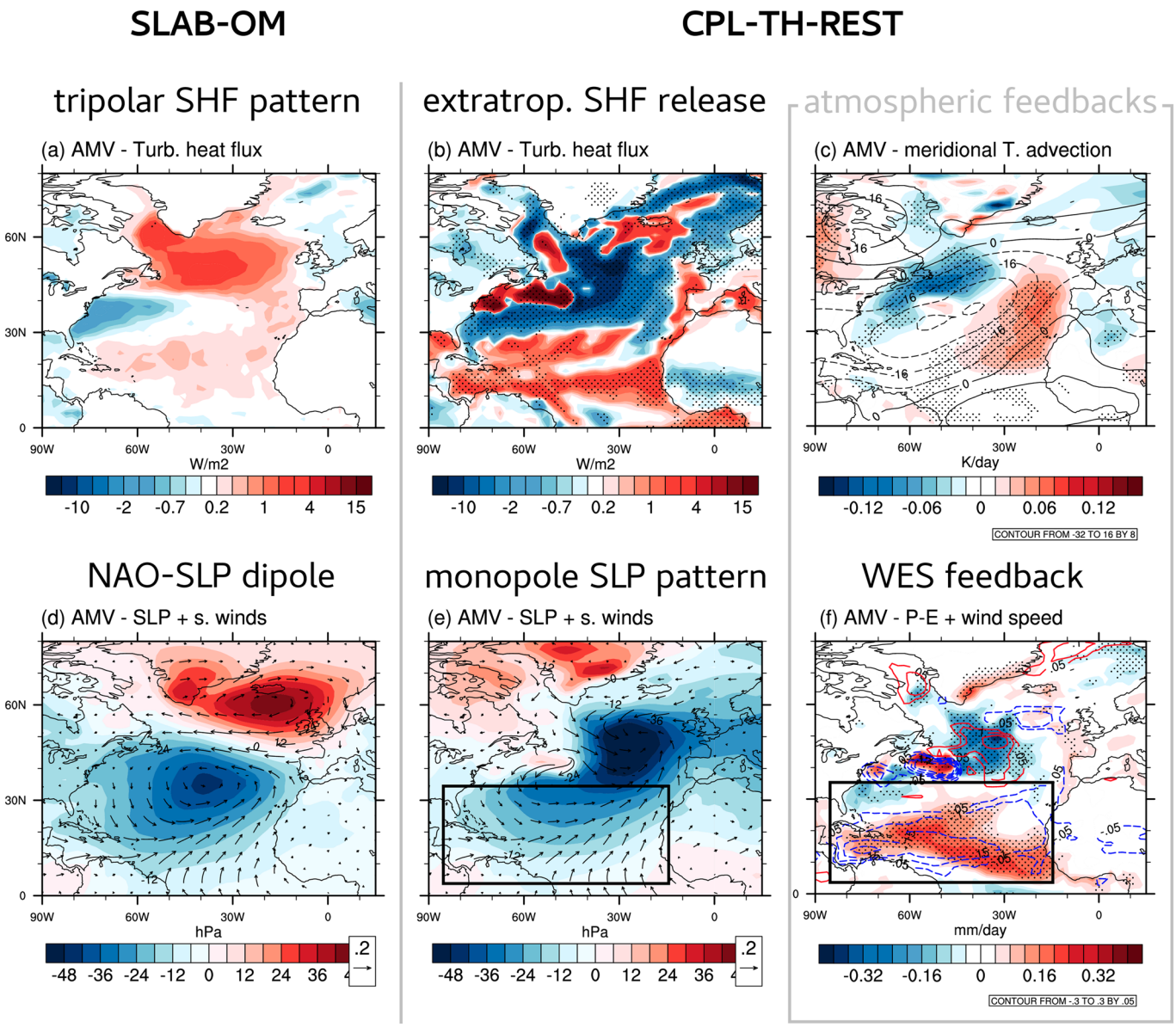

Figure 4. Atmospheric contributions to AMV in the SLAB-OM and CPL-TH-REST experiments. (a, b) Annual turbulent heat flux anomalies as regressions relative to 1 standard deviation change in AMV (W/m^2). The nonlinear scale emphasizes tropical/subtropical heat flux contributions. Pattern are given at Lag 0 (for CPL-TH-REST) and when AMV lags the SHFs by one year (for SLAB-OM). (c) Annual meridional atmospheric temperature advection regression maps relative to 1 standard deviation change in AMV at 850 hPa. The advection term is defined as the product of annual meridional velocity anomalies v' and the mean meridional temperature gradient $v' \frac{\partial \bar{\theta}}{\partial y}$. Units are in K/day and reversed to denote warm-air advection as positive. Contours in (c) denote streamfunction anomalies (10^4 m^2/s) at 850 hPa as regressions on AMV. (d, e) Same as in (a) and (b) but for annual SLP (shading, hPa) and surface wind anomalies (m/s). (f) Same for precipitation minus evaporation (shadings) and surface wind speed anomalies (contours, dashed for negative values). The black boxes mark the tropical branch of AMV, which is dominated by atmospheric feedbacks. Stippling shows significant values for (a)–(c) and (f) (section 2.5).

the similarities of SLP and wind pattern for the coupled and slab-ocean experiments in subtropical and tropical regions. However, unlike short persistence of the AMV-SST signal in SLAB-OM, the tropical AMV-SST branch in the coupled setup has the same intrinsic time scale as the AMOC oscillations. Thus, we argue that multidecadal AMOC variations synchronize atmospheric feedbacks (e.g., WES) on long time scales. Another closely related adjustment process of the large-scale atmospheric circulation to the ocean-driven differential heating is the northward migration of the Intertropical Convergence Zone as underlined by the anomalous P-E band (Figure 4b). This has been generally attributed to AMV (Hodson et al., 2010; Ruprich-Robert et al., 2017; Ting et al., 2011) and, as in this case, to multidecadal AMOC variability (Zhang & Delworth, 2005).

In addition to the WES feedback, which results from air/sea interaction, atmospheric heat transport regionally complements the ocean heat supply. In accordance with theory (linearized quasigeostrophic thermodynamic energy equation; Hoskins & Karoly, 1981), midlatitude ocean heating is balanced by atmospheric horizontal heat advection. We show regressions of the meridional atmospheric heat advection component at 850 hPa, which appears to dominate the zonal component in amplifying the basin-wide warming. Consistent with the anomalous cyclonic lower tropospheric atmospheric circulation, warm-subtropical air is advected toward the eastern extratropical NA, while polar inflow balances warming in the western subpolar NA (Figure 4c). We suggest this increased atmospheric heat transport to regionally increase SSTs in the eastern subtropical and extratropical Atlantic. This is furthermore reflected by positive sensible heat flux anomalies in this region (not shown).

Further positive feedback loops were described to contribute to the tropical arm of AMV. Yuan et al. (2016) emphasized the role of low cloud and dust feedbacks to amplify tropical SST responses. These feedback effects were suggested to originate from precedent warm SSTs and weak trade wind speeds and to substantially alter the radiative balance in the tropics. Nevertheless, Yuan et al. (2016) equally assumed the WES feedback as the primary mechanism of southward propagation of SLP and SST anomalies and is thus in our understanding the main cause of the tropical AMV branch.

Our results show that both effects, the WES feedback and anomalous atmospheric heat advection, are crucial to generate AMV in the dynamic ocean mechanism because they supplement the warming driven directly by the ocean (Figures 4c and 4f). Most notably, they are tightly locked to AMOC/AMV variations, which emphasizes the necessity and inclusion of dynamic ocean circulation and ocean-atmosphere coupling to capture the full evolution of internal AMV.

6. Discussion and Conclusions

In this study, we provide new evidence that long-term AMOC-related SHF changes force atmospheric circulation anomalies to jointly generate AMV. Using coupled and ocean-only simulations with the same model, we disentangle ocean and atmospheric forcing cooperating in the dynamic ocean mechanism. Slow ocean heat convergence is needed to maintain multidecadal persistence of the AMV-SST response (Zhang, 2017) and drives SHF release in the extratropical North Atlantic. Associated trade wind weakening, WES feedback effects and atmospheric heat transport communicate the thermal signal to tropical/subtropical regions and are crucial ingredients for the full response. Even though these feedbacks are partially consistent with related processes acting in the SLAB-OM experiment, extratropical heat sources are controlled by different dynamics with different intrinsic time scales. In addition to previously described key indicators (e.g., SST and upper ocean heat content dipoles Zhang, 2017), we conclusively distinguish these oceanic and atmospheric mechanisms according to their specific large-scale atmospheric circulation signatures. While dipolar SLP anomalies indicate interannual atmospheric NAO forcing in the SLAB-OM experiment, the basin-wide monopole SLP pattern in CPL-TH-REST is well founded by observations (Sutton & Hodson, 2005) and modeling results (Msadek et al., 2011; Ruprich-Robert et al., 2017) to reflect the actual multidecadal atmospheric fingerprint of AMV. Because our highly idealized setup inherently exposes this coherent response to AMOC variability in the multidecadal frequency regime, we reject interpretation of short term, interannual variability (Clement et al., 2015) as the central driver of AMV. The results are therefore essential for our mechanistic understanding of AMV as a coupled ocean-atmosphere mode of variability with the AMOC as a major driver.

Acknowledgments
R. H. was funded by the German Ministry of Education and Research (BMBF) through the MIKLIP project (FKZ: 01LP1517B). L. B. was supported by the BMBF under the Miklip FlexForDec Project (Grant 01LP1519A) and by the European Union under Horizon2020 Project EUCP (Grant Agreement 776613). J. H. J. acknowledges support from the BMBF project RACE-II (FKZ: 03F0729D). J. B. was funded by the Deutsche Forschungsgemeinschaft (DFG, German Research Foundation) under Germany's Excellence Strategy EXC 2037 'CLICCS-Climate, Climatic Change, and Society' Project: 390683824, contribution to the Center for Earth System Research and Sustainability (CEN) of Universität Hamburg. Model output and configuration files can be accessed here (https://cera-www.dkrz.de/WDCC/ui/cerasearch/entry?acronym=DKRZ_LTA_033_ds00004). The authors thank Helmuth Haak and Oliver Gutjahr for their technical support and comments and the two anonymous reviewers, whose comments greatly improved the manuscript.

References

Ba, J., Keenlyside, N. S., Latif, M., Park, W., Ding, H., Lohmann, K., et al. (2014). A multi-model comparison of Atlantic multidecadal variability. *Climate Dynamics*, *43*(9-10), 2333–2348. https://doi.org/10.1007/s00382-014-2056-1

Ba, J., Keenlyside, N. S., Park, W., Latif, M., Hawkins, E., & Ding, H. (2013). A mechanism for Atlantic multidecadal variability in the Kiel Climate Model. *Climate Dynamics*, *41*(7-8), 2133–2144. https://doi.org/10.1007/s00382-012-1633-4

Benjamini, Y., & Hochberg, Y. (1995). Controlling the false discovery rate: A practical and powerful approach to multiple testing. *Journal of the Royal Statistical Society Series B (Methodological)*, *57*(1), 289–300. https://doi.org/10.2307/2346101

Booth, BenB. B., Dunstone, N. J., Halloran, P. R., Andrews, T., & Bellouin, N. (2012). Aerosols implicated as a prime driver of twentieth-century North Atlantic climate variability. *Nature*, *484*(7393), 228–232. https://doi.org/10.1038/nature10946

Borchert, L. F., Dsterhus, A., Brune, S., Müller, W. A., & Baehr, J. (2019). Forecast-oriented assessment of decadal hindcast skill for North Atlantic SST. *Geophysical Research Letters*, *46*, 11,444–11,454. https://doi.org/10.1029/2019GL084758

Borchert, L. F., Müller, W. A., & Baehr, J. (2018). Atlantic ocean heat transport influences interannual-to-decadal surface temperature predictability in the North Atlantic region. *Journal of Climate*, *31*(17), 6763–6782. https://doi.org/10.1175/JCLI-D-17-0734.1

Cane, M. A., Clement, A. C., Murphy, L. N., & Bellomo, K. (2017). Low-pass filtering, heat flux, and Atlantic multidecadal variability. *Journal of Climate*, *30*(18), 7529–7553. https://doi.org/10.1175/JCLI-D-16-0810.1

Chiang, J. C. H., & Bitz, C. M. (2005). Influence of high latitude ice cover on the marine intertropical convergence zone. *Climate Dynamics*, *25*(5), 477–496. https://doi.org/10.1007/s00382--005--0040--5

Clement, A., Bellomo, K., Murphy, L. N., Cane, M. A., Mauritsen, T., Rädel, G., & Stevens, B. (2015). The Atlantic Multidecadal Oscillation without a role for ocean circulation. *Science (New York, N.Y.)*, *350*(6258), 320–324. https://doi.org/10.1126/science.aab3980

Clement, A., Cane, M. A., Murphy, L. N., Bellomo, K., Mauritsen, T., & Stevens, B. (2016). Response to comment on The Atlantic Multidecadal Oscillation without a role for ocean circulation. *Science (New York, N.Y.)*, *352*(6293), 1527. https://doi.org/10.1126/science.aaf2575

Czaja, A., van der Vaart, P., & Marshall, J. (2002). A diagnostic study of the role of remote forcing in tropical atlantic variability. *Journal of Climate*, *15*(22), 3280–3290. https://doi.org/10.1175/1520-0442(2002)015<3280:ADSOTR>2.0.CO;2

Danabasoglu, G. (2008). On multidecadal variability of the Atlantic Meridional Overturning Circulation in the Community Climate System Model Version 3. *Journal of Climate*, *21*(21), 5524–5544. https://doi.org/10.1175/2008JCLI2019.1

Delworth, T. L., & Greatbatch, R. J. (2000). Multidecadal thermohaline circulation variability driven by atmospheric surface flux forcing. *Journal of Climate*, *13*(9), 1481–1495. https://doi.org/10.1175/1520-0442(2000)013

Delworth, T. L., Manabe, S., & Stouffer, R. J. (1993). Interdecadal variations of the thermohaline circulation in a coupled ocean-atmosphere model. *Journal of Climate*, *6*(11), 1993–2011. https://doi.org/10.1175/1520-0442(1993)006

Delworth, T. L., & Zeng, F. (2016). The impact of the North Atlantic Oscillation on climate through its influence on the Atlantic Meridional Overturning Circulation. *Journal of Climate*, *29*(3), 941–962. https://doi.org/10.1175/JCLI-D-15-0396.1

Delworth, T. L., Zeng, F., Zhang, L., Zhang, R., Vecchi, G. A., & Yang, X. (2017). The central role of ocean dynamics in connecting the North Atlantic Oscillation to the extratropical component of the Atlantic Multidecadal Oscillation. *Journal of Climate*, *30*(10), 3789–3805. https://doi.org/10.1175/JCLI-D-16-0358.1

Eden, C., & Jung, T. (2001). North Atlantic interdecadal variability: Oceanic response to the North Atlantic Oscillation (1865–1997). *Journal of Climate*, *14*(5), 676–691. https://doi.org/10.1175/1520-0442(2001)014

Frankignoul, C., Gastineau, G., & Kwon, Y.-O. (2013). The influence of the AMOC variability on the atmosphere in CCSM3. *Journal of Climate*, *26*(24), 9774–9790. https://doi.org/10.1175/JCLI-D-12-00862.1

Gastineau, G., & Frankignoul, C. (2015). Influence of the North Atlantic SST variability on the atmospheric circulation during the twentieth century. *Journal of Climate*, *28*(4), 1396–1416. https://doi.org/10.1175/JCLI-D-14-00424.1

Ghosh, R., Müller, W. A., Baehr, J., & Bader, J. (2017). Impact of observed North Atlantic multidecadal variations to european summer climate: A linear baroclinic response to surface heating. *Climate Dynamics*, *48*(11-12), 3547–3563. https://doi.org/10.1007/s00382-016-3283-4

Giorgetta, M. A., Jungclaus, J., Reick, C. H., Legutke, S., Bader, J., Böttinger, M., et al. (2013). Climate and carbon cycle changes from 1850 to 2100 in MPI-ESM simulations for the Coupled Model Intercomparison Project phase 5. *Journal of Advances in Modeling Earth Systems*, *5*, 572–597. https://doi.org/10.1002/jame.20038

Gulev, S. K., Latif, M., Keenlyside, N., Park, W., & Koltermann, K. P. (2013). North Atlantic Ocean control on surface heat flux on multidecadal timescales. *Nature*, *499*(7459), 464–467. https://doi.org/10.1038/nature12268

Hand, R., Bader, J., Matei, D., Ghosh, R., & Jungclaus, J. H. (2020). Changes of decadal SST variations in the subpolar North Atlantic under strong CO_2 forcing as an indicator for the ocean circulation's contribution to Atlantic multidecadal variability. *Journal of Climate*, *33*(8), 3213–3228. https://doi.org/10.1175/JCLI-D-18-0739.1

Hodson, DanielL. R., Sutton, R. T., Cassou, C., Keenlyside, N., Okumura, Y., & Zhou, T. (2010). Climate impacts of recent multidecadal changes in Atlantic Ocean sea surface temperature: A multimodel comparison. *Climate Dynamics*, *34*(7-8), 1041–1058. https://doi.org/10.1007/s00382-009-0571-2

Hoskins, B. J., & Karoly, D. J. (1981). The steady linear response of a spherical atmosphere to thermal and orographic forcing. *Journal of the Atmospheric Sciences*, *38*(6), 1179–1196. https://doi.org/10.1175/1520-0469(1981)038<1179:TSLROA>2.0.CO;2

Jungclaus, J. H., Fischer, N., Haak, H., Lohmann, K., Marotzke, J., Matei, D., et al. (2013). Characteristics of the ocean simulations in the Max Planck Institute Ocean Model (MPIOM) the ocean component of the MPI-Earth system model. *Journal of Advances in Modeling Earth Systems*, *5*, 422–446. https://doi.org/10.1002/jame.20023

Jungclaus, J. H., Haak, H., Latif, M., & Mikolajewicz, U. (2005). Arctic–North Atlantic Interactions and multidecadal variability of the meridional overturning circulation. *Journal of Climate*, *18*(19), 4013–4031. https://doi.org/10.1175/JCLI3462.1

Knight, J. R. (2005). A signature of persistent natural thermohaline circulation cycles in observed climate. *Geophysical Research Letters*, *32*, 270. https://doi.org/10.1029/2005GL024233

Kushnir, Y. (1994). Interdecadal variations in North Atlantic sea surface temperature and associated atmospheric conditions. *Journal of Climate*, *7*(1), 141–157. https://doi.org/10.1175/1520-0442(1994)007

Kushnir, Y., & Held, I. M. (1996). Equilibrium atmospheric response to north atlantic sst anomalies. *Journal of Climate*, *9*(6), 1208–1220. https://doi.org/10.1175/1520-0442(1996)009<1208:EARTNA>2.0.CO;2

Li, L., Lozier, M. S., & Buckley, M. W. (2020). An investigation of the ocean's role in Atlantic multidecadal variability. *Journal of Climate*, *33*(8), 3019–3035. https://doi.org/10.1175/JCLI-D-19-0236.1

Mauritsen, T., Bader, J., Becker, T., Behrens, J., Bittner, M., Brokopf, R., et al. (2019). Developments in the MPI-M Earth system model version 1.2 (MPI-ESM1.2) and its response to increasing CO_2. *Journal of Advances in Modeling Earth Systems*, *11*, 998–1038. https://doi.org/10.1029/2018MS001400

Msadek, R., Frankignoul, C., & Li, Laurent, Z. X. (2011). Mechanisms of the atmospheric response to North Atlantic multidecadal variability: A model study. *Climate Dynamics*, *36*(7-8), 1255–1276. https://doi.org/10.1007/s00382-010-0958-0

O'Reilly, C. H., Huber, M., Woollings, T., & Zanna, L. (2016). The signature of low-frequency oceanic forcing in the Atlantic multidecadal oscillation. *Geophysical Research Letters*, *43*, 2810–2818. https://doi.org/10.1002/2016GL067925

Ruprich-Robert, Y., Msadek, R., Castruccio, F., Yeager, S., Delworth, T. L., & Danabasoglu, G. (2017). Assessing the climate impacts of the observed atlantic multidecadal variability using the GFDL CM2.1 and NCAR CESM1 global coupled models. *Journal of Climate*, *30*(8), 2785–2810. https://doi.org/10.1175/JCLI-D-16-0127.1

Schlesinger, M. E., & Ramankutty, N. (1994). An oscillation in the global climate system of period 65–70 years. *Nature*, *367*, 723 EP–. https://doi.org/10.1038/367723a0

Sutton, R. T., & Hodson, DanielL. R. (2005). Atlantic ocean forcing of North American and European summer climate. *Science (New York, N.Y.)*, *309*(5731), 115–118. https://doi.org/10.1126/science.1109496

Ting, M., Kushnir, Y., Seager, R., & Li, C. (2011). Robust features of Atlantic multi-decadal variability and its climate impacts. *Geophysical Research Letters*, *38*, L17705. https://doi.org/10.1029/2011GL048712

Trenberth, K., Zhang, R., & National Center for Atmospheric Research Staff (Eds) (2019). Last modified 10 Jan 2019. "The climate data guide: Atlantic multi-decadal oscillation (AMO)". Retrieved from https://climatedataguide.ucar.edu/climate-data/atlantic-multi-decadal-oscillation-amo

Wilks, D. S. (2006). On field significance and the false discovery rate. *Journal of Applied Meteorology and Climatology*, *45*(9), 1181–1189. https://doi.org/10.1175/JAM2404.1

Wilks, D. S. (2016). The stippling shows statistically significant grid points: How research results are routinely overstated and overinterpreted, and what to do about it. *Bulletin of the American Meteorological Society*, *97*, 2263–2273. https://doi.org/10.1175/BAMS-D-15-00267.1

Wills, RobertC. J., Armour, K. C., Battisti, D. S., & Hartmann, D. L. (2019). Ocean atmosphere dynamical coupling fundamental to the Atlantic multidecadal oscillation. *Journal of Climate*, *32*(1), 251–272. https://doi.org/10.1175/JCLI-D-18-0269.1

Xie, S.-P., & Carton, J. A. (2013). Tropical Atlantic variability: Patterns, mechanisms, and impacts. In *Earth's climate* (pp. 121–142). American Geophysical Union (AGU).

Xie, S.-P., & Philander, S. G. H. (1994). A coupled ocean-atmosphere model of relevance to the ITCZ in the eastern pacific. *Tellus A*, *46*(4), 340–350. https://doi.org/10.1034/j.1600-0870.1994.t01-1-00001.x

Yuan, T., Oreopoulos, L., Zelinka, M., Yu, H., Norris, J. R., Chin, M., et al. (2016). Positive low cloud and dust feedbacks amplify tropical North Atlantic Multidecadal Oscillation. *Geophysical Research Letters*, *43*, 1349–1357. https://doi.org/10.1002/2016GL067679

Zanchettin, D., Bothe, O., Müller, W., Bader, J., & Jungclaus, J. H. (2014). Different flavors of the Atlantic multidecadal variability. *Climate Dynamics*, *42*(1-2), 381–399. https://doi.org/10.1007/s00382-013-1669-0

Zhang, R. (2017). On the persistence and coherence of subpolar sea surface temperature and salinity anomalies associated with the atlantic multidecadal variability. *Geophysical Research Letters*, *44*, 7865–7875. https://doi.org/10.1002/2017GL074342

Zhang, R., & Delworth, T. L. (2005). Simulated tropical response to a substantial weakening of the atlantic thermohaline circulation. *Journal of Climate*, *18*(12), 1853–1860. https://doi.org/10.1175/JCLI3460.1

Zhang, R., Sutton, R., Danabasoglu, G., Delworth, T. L., Kim, W. M., Robson, J., & Yeager, S. G. (2016). Comment on "The Atlantic Multidecadal Oscillation without a role for ocean circulation". *Science (New York, N.Y.)*, *352*(6293), 1527. https://doi.org/10.1126/science.aaf1660

Zhang, R., Sutton, R., Danabasoglu, G., Kwon, Y. O., Marsh, R., Yeager, S. G., Amrhein, D. E., & Little, C. M. (2019). A review of the role of the Atlantic Meridional Overturning Circulation in Atlantic Multidecadal Variability and associated climate impacts. *Reviews of Geophysics*, *57*, 316–375. https://doi.org/10.1029/2019RG000644

Zhang, J., & Zhang, R. (2015). On the evolution of Atlantic Meridional Overturning Circulation Fingerprint and implications for decadal predictability in the North Atlantic. *Geophysical Research Letters*, *42*, 5419–5426. https://doi.org/10.1002/2015GL064596